Applied Catalysis B: Environmental 188 (2016) 360–366

Contents lists available at ScienceDirect

Applied Catalysis B: Environmental

journal homepage: www.elsevier.com/locate/apcatb

Differences in photoelectrocatalytic inactivation processes between *E. coli* and its isogenic single gene knockoff mutants: Destruction of membrane framework or associated proteins?

Taicheng An[a,b,*], Hongwei Sun[a,e], Guiying Li[a,b], Huijun Zhao[c], Po Keung Wong[d,**]

[a] The State Key Laboratory of Organic Geochemistry and Guangdong Key Laboratory of Environmental Protection and Resources Utilization, Guangzhou Institute of Geochemistry, Chinese Academy of Sciences, Guangzhou 510640, China
[b] Institute of Environmental Health and Pollution Control, School of Environmental Science and Engineering, Guangdong University of Technology, Guangzhou 510006, China
[c] Centre for Clean Environment and Energy, Griffith University, Gold Coast Campus, QLD, 4222, Australia
[d] School of Life Sciences, The Chinese University of Hong Kong, Shatin, NT, Hong Kong Special Administrative Region, China
[e] University of Chinese Academy of Sciences, Beijing 100049, China

ARTICLE INFO

Article history:
Received 2 November 2015
Received in revised form 29 January 2016
Accepted 4 February 2016
Available online 6 February 2016

Keywords:
Photocatalytic
Fatty acid
Respiration rate
ATP generation potential
Membrane associated protein

ABSTRACT

Fatty acids (FAs) are the main components of bacterial cell membranes (phospholipid bilayer). FA profiles and responses to photoelectrocatalytic (PEC) treatment were comparatively investigated using an *Escherichia coli* parental strain BW25113 and two isogenic FA synthesis deficient mutants. Both mutants, which have higher ratios of unsaturated FAs (UFAs) to saturated FAs (SFAs), were more susceptible to PEC inactivation than the parental strain. PEC treatment can elevate the proportion of bacterial SFA, especially for the mutants, indicating that UFAs are more sensitive to PEC treatment. Collective data from the cytoplasmic K^+ leakage, bacterial fluorescent, and scanning electron microscopic analyses showed that the cytoplasmic membrane framework was damaged by PEC treatment. Interestingly, compared with the membrane framework damage, the functional disruption of membrane proteins was observed much earlier. For example, significant decreases in bacterial respiration rates and adenosine triphosphate (ATP) generation potential were seen in the initial stage of PEC treatment. As such, the disruption of the bacterial energy metabolism system caused by membrane protein damage was more likely the initial lethal step during PEC bacterial inactivation. The clear understanding of PEC inactivation mechanisms can help its practical applications.

1. Introduction

Photocatalytic (PC) and photoelectrocatalytic (PEC) technologies have been studied extensively, and their applications to water disinfection are promising due to the solar energy-driven potential and self-cleaning capacity [1–5]. PC and PEC bacterial inactivation processes do not produce carcinogenic byproducts during disinfection, like conventional processes like chlorination do [6]. However, PC and PEC treatment inactivation mechanisms are still not well established, which hinders the development of mechanism-based kinetic models, as well as practical applications. The bactericidal agents produced in PC and PEC systems include different reactive species (RSs) such as H_2O_2, $O_2^{\bullet -}$, h^+, and $^{\bullet}OH$ [7,8], however, the targets of the RS attacks and the specific lethal steps of PC and PEC treatments are not well understood. For Gram negative bacteria, the outer membrane, cell wall, and cytoplasmic membrane are located at the outside of the cell, and thus are the most probable targets of attack. The damaged bacterial envelopes seen in SEM (scanning electron microscopic) and TEM (transmission electron microscopic) images of PC and PEC treated samples support this hypothesis [9–12].

Some reports have argued that the cell wall is rather porous and might allow RSs to pass through, making this layer not the actual initial attack target [13]. On the other hand, the bacterial cytoplasmic membrane, consisting mainly of the phospholipid bilayer, has been shown to be susceptible to RSs attack, and the oxidative

* Corresponding author at: The State Key Laboratory of Organic Geochemistry and Guangdong Key Laboratory of Environmental Protection and Resources Utilization, Guangzhou Institute of Geochemistry, Chinese Academy of Sciences, Guangzhou 510640, China.
** Corresponding author.
E-mail addresses: antc99@gig.ac.cn, antc99@gdut.edu.cn (T. An), pkwong@cuhk.edu.hk (P.K. Wong).

http://dx.doi.org/10.1016/j.apcatb.2016.02.014
0926-3373/

damage to the cytoplasmic membrane may alter its permeability. This leads to the entry of RSs into intracellular compartments as well as cytoplasmic component leakage [14–16]. However, whether the cytoplasmic membrane framework (phospholipid bilayer) is the initial lethal target of RSs attack during PC and PEC inactivation is still debated.

Additionally, different proteins associated with the cytoplasmic membrane (phospholipid bilayer) play essential roles in various cellular functions, such as substrate transportation and energy metabolism. For example, the electron transport chain for bacterial respiration, including dehydrogenase and a series of coenzymes, is located at the bacterial cytoplasmic membrane [17]. Similar to the cytoplasmic membrane framework, these membrane proteins are also exposed to RSs attack during PC and PEC treatments [1]. Some research suggests that the oxidative damage of these proteins may be essential steps of bacterial inactivation [18]. Nevertheless, the impact of cytoplasmic membrane destruction and membrane protein disruption on bacterial inactivation has not been widely studied during PC or PEC treatment. Thus, it is not clear whether the two types of damage mechanisms mentioned above are lethal steps during PC and PEC inactivation.

This work explored the progression of bacterial membrane changes, to better understand the lethal steps of bacterial inactivation during PEC treatment. The study used an *Escherichia coli* parental strain and its two isogenic mutants; these were effective in studying disinfection mechanisms [19]. Therefore, in this work, the *E. coli* isogenic mutants deficient in fatty acid (most important content of membrane framework) synthesis, together with their parental strain *E. coli* BW25113, were used to investigate the cytoplasmic membrane lipid oxidation mechanism. Does the cytoplasmic membrane oxidative damage occur? Which is the major target of RSs attack, the cytoplasmic membrane framework (phospholipid bilayer) or the membrane associated proteins? Is the decomposition of the cytoplasmic membrane framework or the disruption of membrane associated proteins directly responsible for the bacterial inactivation? Answering these questions would deepen our understanding of PC and PEC disinfection mechanism and further help to develop new high efficiency bactericidal techniques.

2. Experimental section

2.1. Photoelectrocatalytic inactivation apparatus setup

A PEC reactor (50 mL volume) was used [20] to perform inactivation experiments, with a TiO_2 nanotube array photoanode [21]. Detailed experimental conditions are described below; materials included a counter electrode, platinum foil; reference electrode, saturated Ag/AgCl; bias potential of the anode, 1 V *versus* Ag/AgCl; light source, LED lamp with maximum emission at 365 nm and the light intensity adjusted to 27 mW cm^{-2}.

2.2. E. coli *strains and bacterial suspension preparation for inactivation*

Table S1 lists the three *E. coli* strains used for PEC inactivation. All three strains were purchased from Coli Genetic Stock Center (CGSC, Yale University, New Haven, CT, USA). *E. coli* JW3935-4 (Δ*fabR*) and *E. coli* JW1077-1 (Δ*fabH*) were the isogenic mutants of parental strain *E. coli* BW25113 with single gene knocked out. The *fabR* encodes the transcription inhibitor of *fabA* and *fabB*, both of which are essential for unsaturated fatty acid (UFA) synthesis, and the *fabR* deficient strain has elevated UFA fraction compared with wild type strain [22]. The *fabH* encodes β-ketoacyl-acyl carrier protein

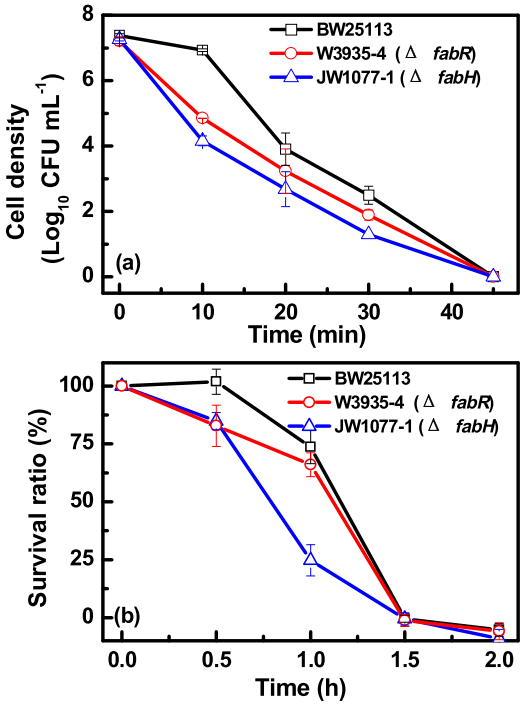

Fig 1. The PEC inactivation performances of parental strain *E. coli* BW25113 and isogenic mutants deficient in fatty acid biosynthesis (*E. coli* JW3935-4 and *E. coli* JW1077-1). (a) The initial bacterial density of the suspension is ~2×10^7 CFU mL^{-1}, and the survived bacteria determined by the colony counting method; (b) the initial bacterial density of the suspension is ~2×10^8 CFU mL^{-1}, and the cell viability determined by Live/Dead Fluorescent Kit.

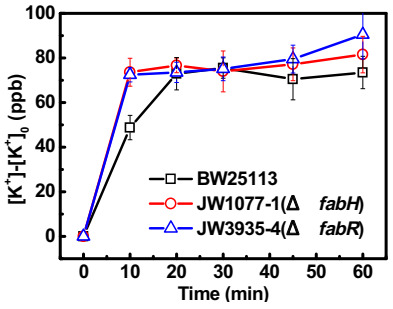

Fig. 2. K^+ leakage from bacterial cells during PEC inactivation (~2×10^7 CFU mL^{-1}) of parental strain *E. coli* BW25113 and two isogenic mutants. The $[K^+]$ represented the K^+ concentration at sampling time point, and $[K^+]_0$ represented the K^+ concentration at time of 0 min for each bacterial strain.

synthase III (KAS III), which catalyzes the condensation reaction during the initial step of fatty acid biosynthesis [23].

Previous studies found that the KAS III deficient *E. coli* strain had a higher UFA proportion compared with the wild type strain, especially the monounsaturated fatty acid with 18 carbons (18:1) [24]. The bacterial strains were stored in 25% sterilized glycerin at −80 °C. To prepare the bacterial suspension for PEC inactivation, the individual bacterial strain was streaked on a nutrient agar plate and incubated to acquire isolated colonies. The colony was inoculated into Nutrient Broth (NB) and incubated overnight. The bacterial suspension was diluted with fresh NB by 1:100, and then incubation continued for 6 h at 37 °C and 200 rpm to log phase. The bacterial cells were harvested by centrifugation at 5000 rpm for 5 min, washed twice with sterilized water, and re-suspended in 0.2 M $NaNO_3$. Unless otherwise noted, the bacterial density of the suspension used for PC and PEC inactivation in this study was ~2×10^7 CFU mL^{-1} (colony forming unit per mL).

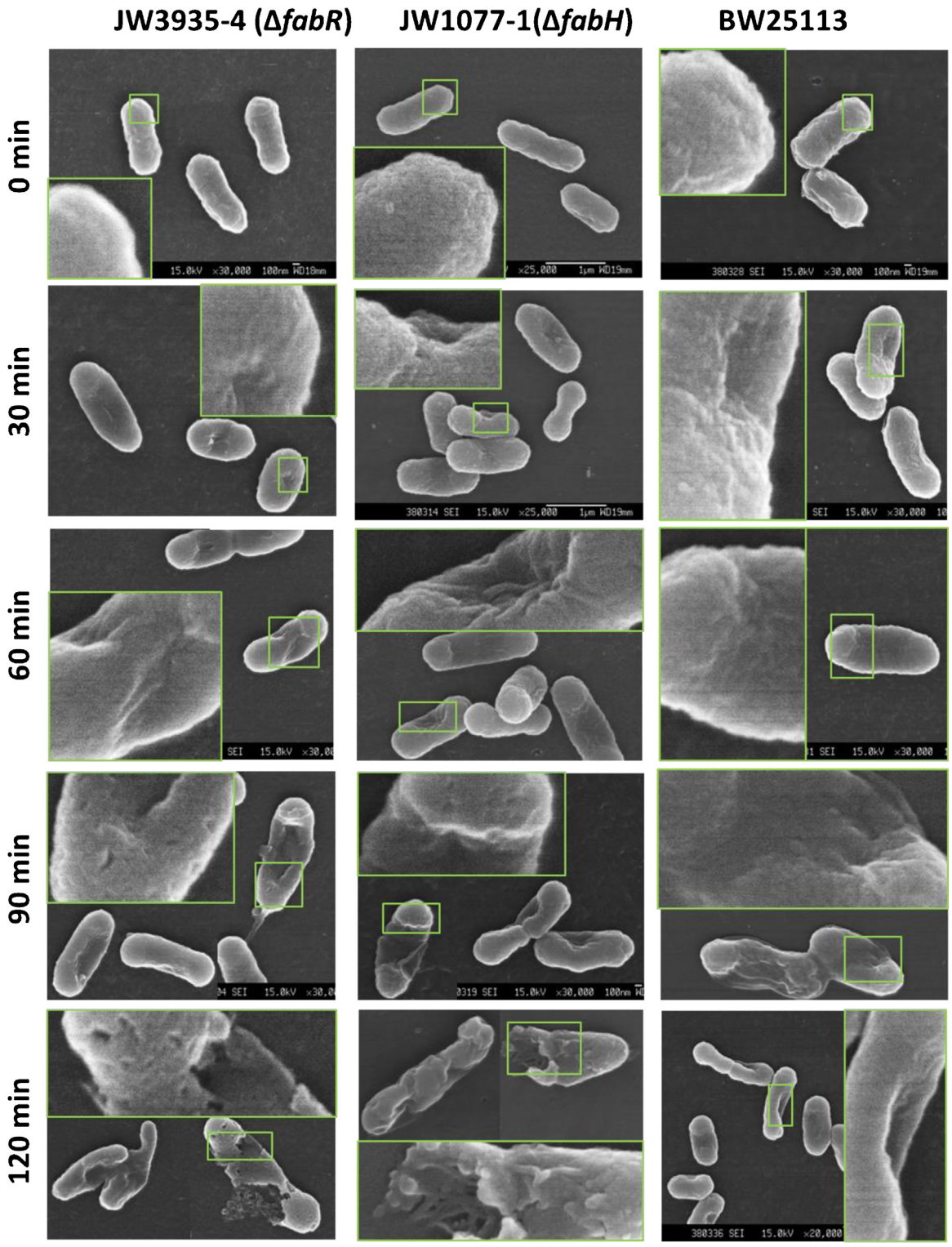

Fig. 3. The SEM images of cell samples during PEC inactivation (~2×10^7 CFU mL^{-1}, the parental strain *E. coli* BW25113 and two isogenic mutants).

2.3. PEC inactivation

PEC treatment was applied to 50 mL of the bacterial suspension prepared above; surviving bacterial cells were monitored using a colony counting method [21]. The bacterial viability was also tested using a Live/Dead Backlight Bacterial Viability Kit (L13152, Invitrogen, USA), following the manufacturer's instructions.

2.4. Fatty acid (FA) profile analysis

The FA profiles of three *E. coli* strains were determined as follows [11,12]: the bacteria in the log phase were harvested and washed; 2 mL 5% NaOH solution (methanol: H_2O = 1:1, v:v) was then added. The mixture was saponificated in 100 °C for 30 min; and the pH was adjusted to 2 using 6 M HCl. The mixture was extracted twice with 5 mL of mixed solvent (Hexane: chloroform = 4:1). The extract

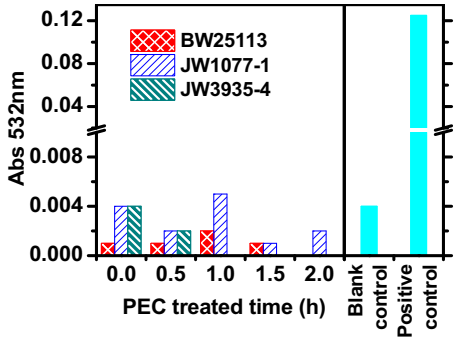

Fig. 4. The lipid peroxidation levels of bacterial membrane for parental strain *E. coli* BW25113, isogenic mutants *E. coli* JW3935-4 (Δ*fabR*) and *E. coli* JW1077-1 (Δ*fabH*) during PEC inactivation processes (bacterial density is ~2×10^8 CFU mL^{-1}). Blank control: alcohol was used instead of samples for the assay; positive control: MDA standard solution of 10 nmol mL^{-1} was used instead of samples for the assay; both controls was conducted in the same procedure as the bacterial samples, following the manufacturer's instruction.

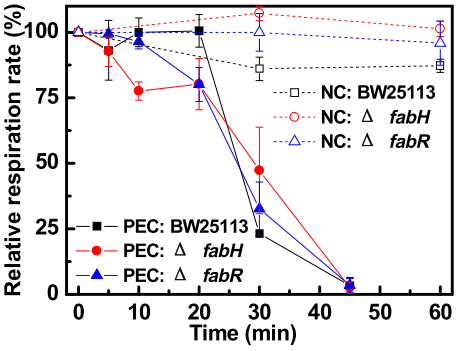

Fig. 5. The bacterial respiration rate assays of parental strain *E. coli* BW25113 and two isogenic mutants (Δ*fabR* and Δ*fabH*) during PEC inactivation (~2×10^8 CFU mL^{-1}). NC: negative control.

was then dried with a gentle nitrogen flow. Methylation was conducted at 100 °C for 30 min by adding 4 mL 14% BF_3 in methanol. The sample was extracted twice with 5 mL of the same mixed solvent, evaporated until dry, and then finally resolved in 200 μL hexane. The fatty acid components were analyzed using an Agilent 7890A-5975C GC–MS; the quantification was conducted using calibration curves of fatty acid methyl ester standards from Accustandard (125 Market Street, New Haven, CT 06513, USA). The PEC inactivated bacterial cultures (2×10^8 CFU mL^{-1}) were collected using filtration and the fatty acid profile was analyzed using the same procedure as above.

2.5. K^+ leakage and fluorescent microscopic observation

Bacterial cultures were filtered to remove cells; the K^+ concentration in the filtrate was tested using inductively coupled plasma-atomic emission spectroscopy (VARIAN VISTA ICP-AES Pro, USA) at 766.5 nm. Fluorescent images of bacterial samples were taken after being stained with a Live/Dead Backlight bacterial viability kit, following the manufacturer's instructions.

2.6. Field emission scanning electron microscope (FESEM) images and lipid peroxidation assay

Bacterial cultures for SEM observation were prepared as follows [25]: bacteria were harvested and fixed with 2.5% glutaraldehyde overnight, and then soaked with 0.1% phosphate-buffered saline 5 times each for 20 min. Dehydration was performed in turn using 30, 50, 70, 90, 100% ethanol and 100% butyl alcohol. After being freeze dried and gold sputtered, the images were taken with FESEM (JSM-6330F, JEOL Ltd., Japan). The lipid peroxidation level was determined by testing the malonaldehyde (MDA) concentration using a MDA assay kit (A003-1, Nanjing Jiancheng Bioengineering Institute). MDA reacts with thiobarbituric acid (TBA) to form a pink product with a maximum absorbance of 532 nm [11,26,27].

2.7. Bacterial respiration activity assay

The bacterial respiration rate was tested using 2,3,5-triphenyltetrazoliumchloride (TTC) as follows [16]: 8 mL of PEC treated bacterial samples (2×10^8 CFU mL^{-1}) were harvested using filtration, and re-suspended in 1 mL phosphate buffer saline (PBS, pH = 7.4). Then, 0.75 mL tris(hydroxymethyl) aminomethane-HCl buffer (Tris-HCl, pH = 8.4), 0.25 mL 0.36% $NaSO_3$, 40 μL 1 M glucose and 1 mL 0.4% TTC (Cat No. 118388, J&K Scientific Ltd.) were added. The reaction mixture was incubated at 37 °C and 200 rpm for 60 min; 0.5 mL 40% formaldehyde solution was added to terminate the reaction. After being centrifuged at 8000 rpm for 10 min, the deposit was extracted with 3 mL acetone for 10 min, and the absorbance at 485 nm of supernatant was then tested. The principle of the assay was described in the Supporting information (SI) and illustrated in Fig. S1.

2.8. Adenosine triphosphate (ATP) generation potential

A 0.9 mL aliquot bacterial sample was collected at the 0, 5, 10, 15, 20, 25 and 30 min points after the start of PEC inactivation. Each sample was mixed with 0.1 mL sterilized nutrient broth, and incubated at 37 °C. After incubation for 5, 15, 30, 45 and 60 min, the cellular ATP concentration was measured using a BacTiter-Glo™ Microbial Cell Viability Assay Kit (G8230, Promega Corporation, 2800 Woods Hollow Road, Madison, WI 53711–5399, USA), following the manufacturer's instructions with minor modification. A 0.05 mL aliquot sample was mixed with an equal volume of BacTiter-Glo™ reagent in a white opaque-walled 96-well plate, and incubated on an orbital shaker for 5 min at room temperature (*ca.* 25 °C). The luminescence intensity was recorded immediately using a plate reader (Varioskan Flash, Thermo Scientific, USA). A calibration curve was measured using ATP-2Na·3H_2O (AB0020, Sangon Biotech, Shanghai) solutions. Fig. S2 illustrates the ATP assay.

3. Results and discussion

3.1. Fatty acid profile

Fatty acid is the major composite of bacterial membranes, and is present in the form of a phospholipid bilayer and lipopolysaccharide. The phospholipid bilayer builds up the framework of bacterial membrane. Phospholipid consists of saturated fatty acids (SFAs). SFAs are more viscous and less fluid, and therefore tougher and more recalcitrant to oxidative stress [28], than unsaturated fatty acids (UFAs). Therefore, the parental strain *E. coli* BW25113 and two isogenic mutants (*E. coli* JW3935-4 (Δ*fabR*) and *E. coli* JW1077-1 (Δ*fabH*)), which are deficient in fatty acids synthesis, were used to investigate the different behavior patterns of FA during PEC inactivation. The FA profiles of three *E. coli* strains were first determined to confirm the target mutations; Table S2 shows the results. Before PEC treatment, the parental strain *E. coli* BW25113 showed a typical *E. coli* fatty acid profile [16,24], with palmitic acid (16:0) as the dominant congener (45.6%), followed by monounsaturated fatty acids such as hexadecenoic acid (16:1, 12.1%) and octadecenoic acid (18:1, 22.9%). Compared with the parental strain, the mutants showed no difference in aspect of the total fatty acid content, but with different composition profiles. The proportion of SFA (palmitic

Table 1
The ATP generation rate of parental strain *E. coli* BW25113 and its isogenic mutants after PEC inactivation ($\sim 2 \times 10^7$ CFU mL^{-1}) with different treatment times.

PEC time (min)	ΔATP/Δt (10^{-7} pmol min^{-1} per cell)			Percentage (%)		
	BW25113	JW3935-4	JW1077-1	BW25113	JW3935-4	JW1077-1
0	0.62	0.92	0.74	100.0	100.00	100.00
2.5	-	0.88	0.75	-	95.56	100.38
5.0	0.54	0.81	0.04	87.3	87.81	4.82
7.5	-	0.35	0.00	-	38.21	0.00
10	0.20	0.04	0.00	32.7	4.40	0.00
15	−0.01	0.00	0.00	−1.4	0.00	0.00
20	0.00	0.00	0.00	0.6	0.00	0.00
25	0.01	-	-	1.5	-	-
30	0.01	-	-	1.9	-	-

acid) decreased to 37.6% (*E. coli* JW3935-4: Δ*fabR*) and 38.5% (*E. coli* JW1077-1: Δ*fabH*), and the unsaturated fractions elevated to 45.9% (*E. coli* JW3935-4: Δ*fabR*) and 45.7% (*E. coli* JW1077-1: Δ*fabH*), respectively. The results were consistent with previous reports on the gene functions of *fabR* and *fabH*, as well as the phenotype of the deficient strains [22,24].

3.2. PEC inactivation performance

Fig. 1 shows the PEC inactivation performances of different *E. coli* strains, the parental strain, and two isogenic mutants (Δ*fabH* and Δ*fabR*). In a bacterial suspension of 2×10^7 CFU mL^{-1}, *E. coli* BW25113, the parental strain, showed a shoulder region (the survival bacterial population decreased very slowly) during the initial 10 min; the two mutants were inactivated more quickly, and without the shoulder stage. After 10 min of PEC treatment, the survival ratios were >50%, ∼1%, and ∼0.1% for *E. coli* BW25113, *E. coli* JW3935-4, and *E. coli* JW1077-1, respectively. This indicates the mutants with higher UFA proportions were more susceptible to PEC treatment. With further prolonging of treatment time, the live cell population decreased steadily; 100% inactivation was finally achieved within 45 min for all three strains (Fig. 1a).

In addition, the bacterial survival ratios of three bacterial strains (2×10^8 CFU mL^{-1}) were also determined with Live/Dead Backlight Bacterial Viability Kit during the PEC treatment process. Fig. 1b shows that the PEC inactivation efficiency for Δ*fabH* was greater than Δ*fabR*, which was greater than the parental strain. It required 1.5 h for all three strains to achieve complete inactivation. Similar with the results in Fig. 1a, a shoulder stage is seen for the first 0.5 h for *E. coli* BW25113. This test used a higher initial bacterial concentration, leading to a longer time being needed to achieve complete inactivation. Therefore, the parental strain *E. coli* BW25113 with a higher SFA ratio was more resistant to PEC inactivation compared with the mutants. This conclusion also confirms other research that found that the higher the UFA to SFA ratio, the more sensitive the bacteria are to PC inactivation [10,29]. These results suggest that UFA was likely the important initial target of RSs during PC and PEC process, leading to the structural destruction of bacterial membrane framework.

To confirm this hypothesis, the bacterial fatty acid profiles during PEC inactivation processes were compared with the untreated samples. As Table S2 shows, PEC treatment reduces the proportion of UFA, especially for mutants with a higher original UFA content before treatment. For example, the proportion of UFA in *E. coli* JW3935-4 dropped from 45.9% to 28.7% after 2 h of PEC treatment; the corresponding UFA in *E. coli* JW1077-1 decreased from 45.7% to 34.9% during the same treatment period. The results demonstrate that the UFA oxidative damage caused by RSs attack occur during PEC inactivation of *E. coli*.

3.3. Bacterial membrane integrity test

During the PEC treatment process, fatty acid profile changes indicated possible *E. coli* cell membrane damage. Further tests were therefore done to confirm these membrane integrity changes. K^+ is an important ion in cytoplasm, and the destruction of bacterial membrane should induce the leakage of K^+ and cytoplasm [11,21]. As Fig. 2 shows, a sharp increase of K^+ concentration in the bacterial suspension was observed for all three strains within the initial 10 min, implying that membrane permeability increased significantly and early. Specifically, both mutants showed faster K^+ leakage compared with the parental strain, consistent with the inactivation performance.

This reaffirms the importance of bacterial fatty acid profiles in maintaining membrane permeability; the bacterial strain with high UFA fractions was susceptible to oxidative stress caused by PEC treatment. More precisely, the extent of K^+ leakage coincided with the bacterial inactivation ratio for all three strains. For *E. coli* BW25113, the inactivation ratios were 64.66% and 99.95% within 10 and 20 min (Fig. 1a); the corresponding K^+ leakage percentages were 65% and 97%, respectively. Similar results were seen for *E. coli* JW3935-4 (Δ*fabR*) and *E. coli* JW1077-1 (Δ*fabH*). This suggests that the cytoplasmic membrane destruction is an essential initial step for bacterial inactivation.

Cytoplasmic membrane integrity was further monitored using a Live/Dead BacLight™ bacterial viability kit with a fluorescent microscope; bacteria with an intact membrane was stained green, and bacteria with a destroyed membrane was stained red [30,31]. As Fig. S3 shows, for *E. coli* BW25113 cells (2×10^7 CFU mL^{-1}), the color turns from green to red gradually during PEC treatment; all the cells are red within 45 min. However, the bacterial cells of *E. coli* JW3935-4 (Δ*fabR*) and *E. coli* JW1077-1 (Δ*fabH*) were all red after only 30 min of PEC treatment (Fig. S4). The mutant's faster loss of membrane integrity compared with the parental strain further confirmed that membrane FA, especially the UFA fraction, was an important target of RSs attack.

The SEM images of PEC treated bacterial cells were also compared to provide more details about the membrane damage. As Fig. 3 shows, the untreated cells of *E. coli* BW25113 were plump rod shapes with intact membrane. However, after 30 min of PEC treatment, there was sinking in the middle part of some cells, indicating partial cytoplasm leakage. Longer PEC inactivation time led to more severe damage to the bacteria, with more sinking and a shriveled membrane. As noted above, both mutants (Δ*fabR* and Δ*fabH*) with higher UFA fractions were more sensitive to PEC inactivation under identical experimental conditions. After 30 min treatment, most of these cells were sunken in the middle. The cell membrane became porous, and many fine holes were seen on the bacterial membrane after 90 min. Furthermore, significant bacterial cell debris, likely the collapsed cell wall or broken membrane, was seen after 120 min. The SEM results demonstrated clearly that PEC induced the

damage to the cytoplasmic membrane and cell wall; the membrane with more UFA was more easily destroyed.

3.4. Mechanism of membrane destruction

The mechanism of fatty acid damage was further explored. Lipid peroxidation is widely accepted as the damage pathway caused by RSs attack. MDA, a product of lipid peroxidation, was used to indicate this oxidative process [13,16,32,33]. Fig. 4 shows the MDA concentration changes. Interestingly, the MDA concentration did not substantively increase during the 2 h PEC treatment for all three *E. coli* strains, compared with blank control (alcohol instead of bacterial samples for MDA assay). This suggests that PEC inactivation may not cause the elevated lipid peroxidation level, or that the cell membrane lipid was not damaged by lipid peroxidation. However, these results can be explained by the fact that the dominant bactericidal RSs was in-situ generated H_2O_2 rather than •OH [21]. Lipid peroxidation is generally induced by •OH [15]. Further, the major fatty acid contents of three *E. coli* strains were saturated or monounsaturated, whereas the lipid peroxidation processes generally took place with polyunsaturated fatty acids as the substrate [26,34,35]. As such, the mechanism of membrane lipid damage requires further study.

3.5. Bacterial respiration rate measurement

Respiration is an important form of bacterial energy metabolism; released energy is stored as ATP. The bacterial respiratory chain consists of different enzymes, flavoproteins, iron-sulfur proteins, and cytochromes, and is located at the cytoplasmic membrane of bacterial cells [36]. During the PEC inactivation process, RSs may attack the respiratory chain, as well as the cytoplasmic membrane framework (phospholipid bilayer) [37,38]. Therefore, during the PEC inactivation process, bacterial respiration rate changes were tested using TTC reduction experiments. Electrons produced during bacterial respiration reduced TTC to red-colored TF (Fig. S1). The experimental conditions for the TTC assay were first optimized, including the nutrient substrate selection, pH buffer system, and bacterial density and reduction duration, as shown in Figs. S5 and S6 .

The optimization process suggested that adding glucose rather than succinate [39] or nutrient broth as the substrate promoted TTC reduction (Fig. S5). The optimized dose was 40 μL 1 M glucose (total volume of 3 mL, (Fig. S6a); the best buffer solution was Tris-HCl (pH 8.4); and the optimal bacterial density was ~10^9 CFU mL^{-1}. Thus, the bacterial suspension after PEC treatment (~10^8 CFU mL^{-1}) was condensed to ~10^9 CFU mL^{-1} before the TTC assay. The assay was operated for 60 min (Fig. S6b), and calibration curves of TF were obtained (Figs. S6c and d).

Fig. 5 shows the respiration rates of PEC treated bacterial samples based on the optimized conditions. In the negative controls (NC, where no catalyst, UV light, or bias potential was applied), the bacterial respiration rate showed no apparent changes. However, during the PEC process, the respiration rate of two mutants decreased slightly within the initial 20 min, fell sharply thereafter, and then ceased within 45 min. The *E. coli* BW25113 showed a slower fall in respiration than the two mutants. The loss of bacterial respiration activity was probably caused by the oxidative damage of the membrane proteins, which may play an important role in the respiratory chain. When the respiration rates were compared with the bacterial survival ratios under identical PEC conditions (~2×10^8 CFU mL^{-1}, Fig. 1b), the loss of respiration activity was far faster than the loss of bacterial viability. This suggests that some bacteria were partially injured by the lost respiration activity, but did not die. Thus, the oxidative damage of the bacterial respiratory chain occurred at the early stage of PEC inactivation, similar with Bosshard's report of solar disinfection [18].

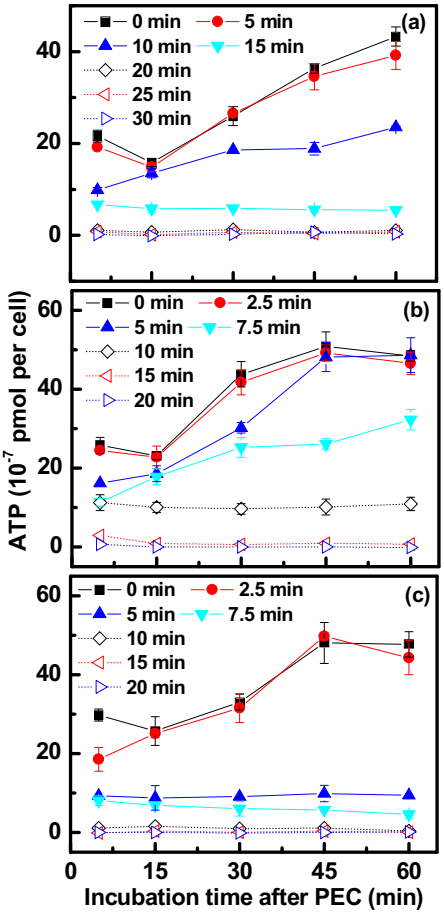

Fig. 6. The ATP generation potential of *E. coli* strains (cell concentration ~2×10^7 CFU mL^{-1}) after PEC inactivation. (a) *E. coli* BW25113, (b) Δ*fabR*, (c) Δ*fabH*. PEC inactivated bacterial samples were mixed with 10% NB and incubated at 37 °C in water bath for indicated times.

3.6. Bacterial ATP generation capacity

The decrease of the respiration rate of bacteria during PEC inactivation reduces the energy production capacity of the nutrient substrates, and subsequently, the generation rate of ATP, which is the cell's major energy currency molecule. Thus, this study also examined bacterial ATP generation capacity during PEC inactivation. The cellular ATP concentration was determined using a BacTiter-Glo™ Microbial Cell Viability Assay. The limit of detection (LOD, defined as the bacterial density to produce Signal/Noise = 3) of the assay was tested following manufacturer instructions, and *E. coli* BW25113 was adopted as the model microorganism. The LOD was calculated to be 2–3 × 10^4 CFU mL^{-1} (Fig. S7a). The luminescence density of the assay was found to decline with prolonged incubation time (Fig. S7b). As such, the sample was tested after 5 min of incubation on the orbital shaker to ensure sufficient mixing.

Fig. 6 shows the ATP concentrations of the bacteria during PEC inactivation and during the following incubation process. For *E. coli* BW25113, the ATP level dropped from 21.6 × 10^{-7} pmol per cell before the inactivation to 9.9 × 10^{-7} pmol per cell after 10 min of PEC treatment, and to 1.1 × 10^{-7} pmol per cell after 20 min (Fig. 6a). When the treated bacterial samples were subsequently incubated with 10% nutrient broth, the cellular ATP level increased, indicating that the cells could still use the nutrition to generate energy.

The ATP level increased more slowly when a longer PEC treatment time was applied, and after 15 min of PEC treatment, the cellular ATP concentration no longer increased with nutrient incubation. This suggests that PEC treatment may gradually damage and finally destroy the bacterial energy generation capacity, including the previously discussed respiration pathway. The ATP levels in two mutants (Δ*fabR* and Δ*fabH*) showed similar trends as the parental strain *E. coli* BW25113, except ATP generation capacity was lost earlier for the two mutants: after 10 min PEC treatment for Δ*fabR* and after 5 min for Δ*fabH* (Fig. 6b and c).

As Table 1 shows, the cellular ATP generation rate (ΔATP/Δt) was also calculated with ATP concentrations at different incubation times of 15, 30, 45, and 60 min. PEC inactivation decreases the cellular ATP generation rate for all three strains. For *E. coli* BW25113, the rate was reduced to 32.7% of the original after 10 min PEC inactivation, and to 0% after 15 min. The *E. coli* BW25113 survival ratio was 35.3% at 10 min, and ~1% at 15 min (Fig. 1a), coinciding with the ATP decrease. The results for Δ*fabR* and Δ*fabH* mutants were similar.

The loss of ATP generation capacity appears to directly cause bacterial death: a lack of ATP limits the cellular energy supply, preventing cellular repair and bacterial growth. Comparatively, the loss in respiration activity did not kill the bacteria, because respiration is not the only way the facultative anaerobic *E. coli* metabolizes energy. ATP can also be generated though fermentation *via* substrate level phosphorylation [40]. The bacterial ATP generation capacity was completely lost only when all the energy metabolism pathways were blocked or the ATP synthase was inactivated. The simultaneous leakage of K^+ along with the bacterial inactivation may be because ATP is needed to maintain both bacterial membrane potential and Na^+-K^+ ATPase [21,38] which were essential to keep K^+ concentration at a high level. In addition, the damage of the cellular outer membrane, including lipid bilayers, may cause increased bacterial permeability. This subsequently increases the exposure probability of the respiratory chain and ATP synthase to RSs. This was demonstrated by comparing the mutants and the parental strain.

4. Conclusion

In summary, this study found that the oxidative damage of membrane associated proteins, particularly those related with the bacterial energy metabolism such as respiration and ATP generation, was the lethal steps in bacterial inactivation during PEC treatment. This can be supported by the observation that the respiration rate decreased more quickly than bacterial viability, as well as that the ATP generation potential coincided with bacterial viability. On the other hand, the ROSs attack also induced oxidative damage of membrane fatty acids, especially the unsaturated content, which subsequently caused elevated membrane permeability. Nevertheless, the damage of membrane framework seemed not as important as membrane proteins, because of its later occurrence compared with protein disruption during bacterial inactivation process. Even though, the permeabilized membrane framework did promote the ROSs attacking membrane proteins, supported by the different performance between parental *E. coli* and fatty acid deficient mutants. The clear understanding of PEC inactivation mechanisms can help us to develop new high efficiency bactericidal techniques.

Acknowledgments

This is contribution No. IS-2185 from GIGCAS. This work was financially supported by National Natural Science Funds for Distinguished Young Scholars (41425015), National Natural Science Foundation of China (41573086 and 41373103), Research Grant Council, Hong Kong SAR Government (GRF476811). P.K. Wong would like to thank the support from CAS/SAFEA International Partnership Program for Creative Research Teams of Chinese Academy of Sciences.

Appendix A. Supplementary data

Supplementary data associated with this article can be found, in the online version, at http://dx.doi.org/10.1016/j.apcatb.2016.02.014.

References

[1] T. Matsunaga, R. Tomoda, T. Nakajima, H. Wake, FEMS Microbiol. Lett. 29 (1985) 211–214.
[2] A.G. Rincon, C. Pulgarin, Catal. Today 122 (2007) 128–136.
[3] W.J. Wang, Y. Yu, T.C. An, G.Y. Li, H.Y. Yip, J.C. Yu, P.K. Wong, Environ. Sci. Technol. 46 (2012) 4599–4606.
[4] P. Gao, J. Liu, D.D. Sun, W. Ng, J. Hazard. Mater. 250 (2013) 412–420.
[5] G.Y. Li, X.L. Liu, H.M. Zhang, T.C. An, S.Q. Zhang, A.R. Carroll, H.J. Zhao, J. Catal. 277 (2011) 88–94.
[6] P. Kulkarni, S. Chellam, Sci. Total Environ. 408 (2010) 4202–4210.
[7] M. Cho, H. Chung, W. Choi, J. Yoon, Water Res. 38 (2004) 1069–1077.
[8] W.J. Wang, L.S. Zhang, T.C. An, G.Y. Li, H.Y. Yip, P.K. Wong, Appl. Catal. B: Environ. 108–109 (2011) 108–116.
[9] H.X. Shi, G.Y. Li, H.W. Sun, T.C. An, H.J. Zhao, P.K. Wong, Appl. Catal. B: Environ. 158 (2014) 301–307.
[10] M.H. Gao, T.C. An, G.Y. Li, X. Nie, H.Y. Yip, H. Zhao, P.K. Wong, Water Res. 46 (2012) 3951–3957.
[11] C. Hu, J. Guo, J.H. Qu, X.X. Hu, Langmuir 23 (2007) 4982–4987.
[12] Y.W. Cheng, R.C.Y. Chan, P.K. Wong, Water Res. 41 (2007) 842–852.
[13] O.K. Dalrymple, E. Stefanakos, M.A. Trotz, D.Y. Goswami, Appl. Catal. B: Environ. 98 (2010) 27–38.
[14] C. Pulgarin, J. Kiwi, V. Nadtochenko, Appl. Catal. B: Environ. 128 (2012) 179–183.
[15] V. Nadtochenko, J. Kiwi, Langmuir 21 (2005) 4631–4641.
[16] O.K. Dalrymple, W. Isaacs, E. Stefanakos, M.A. Trotz, D.Y. Goswami, J. Photochem. Photobiol. A 221 (2011) 64–70.
[17] D.J. Richardson, Microbiology 146 (2000) 551–571.
[18] F. Bosshard, M. Bucheli, Y. Meur, T. Egli, Microbiology 156 (2010) 2006–2015.
[19] H.X. Shi, G.C. Huang, D.H. Xia, T.W. Ng, H.Y. Yip, G.Y. Li, T.C. An, H.J. Zhao, P.K. Wong, J. Phys. Chem. B 119 (2015) 3104–3111.
[20] X. Nie, G.Y. Li, P.K. Wong, H.J. Zhao, T.C. An, Catal. Today 230 (2014) 67–73.
[21] H.W. Sun, G.Y. Li, X. Nie, H.X. Shi, P.K. Wong, H.J. Zhao, T.C. An, Environ. Sci. Technol. 48 (2014) 9412–9419.
[22] Y.M. Zhang, H. Marrakchi, C.O. Rock, J. Biol. Chem. 277 (2002) 15558–15565.
[23] C.Y. Lai, J.E. Cronan, J. Biol. Chem. 278 (2003) 51494–51503.
[24] J.T. Tsay, W. Oh, T.J. Larson, S. Jackowski, C.O. Rock, J. Biol. Chem. 267 (1992) 6807–6814.
[25] G.Y. Li, X.L. Liu, H.M. Zhang, P.K. Wong, T.C. An, H.J. Zhao, Appl. Catal. B: Environ. 140–141 (2013) 225–232.
[26] J. Kiwi, V. Nadtochenko, J. Phys. Chem. B 108 (2004) 17675–17684.
[27] G. Carré, E. Hamon, S. Ennahar, M. Estner, M.-C. Lett, P. Horvatovich, J.-P. Gies, V. Keller, N. Keller, P. Andre, Appl. Environ. Microbiol. (2014), http://dx.doi.org/10.1128/AEM.03995-13AEM.03995-13.
[28] H. Trauble, P. Overath, Biochim. Biophys. Acta 307 (1973) 491–512.
[29] T.Y. Leung, C.Y. Chan, C. Hu, J.C. Yu, P.K. Wong, Water Res. 42 (2008) 4827–4837.
[30] G. Gogniat, M. Thyssen, M. Denis, C. Pulgarin, S. Dukan, FEMS Microbiol. Lett. 258 (2006) 18–24.
[31] O.N. Mileyeva-Biebesheimer, A. Zaky, C.L. Gruden, Environ. Eng. Sci. 27 (2010) 329–335.
[32] J. Kiwi, V. Nadtochenko, Langmuir 21 (2005) 4631–4641.
[33] V.A. Nadtochenko, A.G. Rincon, S.E. Stanca, J. Kiwi, J. Photochem. Photobiol. A 169 (2005) 131–137.
[34] E. Cabiscol, J. Tamarit, J. Ros, Int. Microbiol. 3 (2000) 3–8.
[35] J.A. Imlay, EcoSal Plus 1 (2013).
[36] W.D. Stansfield (Ed.), Schaum's Outline of Theory and Problems of Molecular and Cell Biology, McGraw-Hill Companies, Inc., USA, 1996.
[37] M. Berney, H.-U. Weilenmann, T. Egli, Microbiology 152 (2006) 1719–1729.
[38] F. Bosshard, M. Berney, M. Scheifele, H.U. Weilenmann, T. Egli, Microbiol. SGM 155 (2009) 1310–1317.
[39] P.C. Maness, S. Smolinski, D.M. Blake, Z. Huang, E.J. Wolfrum, W.A. Jacoby, Appl. Environ. Microbiol. 65 (1999) 4094–4098.
[40] D.P. Clark, FEMS Microbiol. Rev. 5 (1989) 223–234.